Adsorption Hysteresis in Porous Solids

M. D. Donohue,[1] and G. L. Aranovich

Department of Chemical Engineering, The Johns Hopkins University, Baltimore, Maryland 21218

Hysteresis has been observed in adsorption isotherms for a number of gas–solid systems and, generally, is attributed to adsorption in mesoporous materials with capillary condensation. This behavior is classified as Type IV or Type V in the IUPAC classification scheme. Here, lattice theory is used to predict adsorption behavior in pores. The Ono–Kondo theory is used with appropriate boundary conditions for fluid adsorption in infinite and semi-finite slit-like pores. It is shown that there can be phase transitions in the adsorbed phase which lead to hysteresis in kinetically controlled experiments. However, hysteresis in equilibrium behavior is exhibited only in pores of finite length. For finite-length pores, the interface geometry is predicted to be different during the processes of adsorption and desorption and this difference in interface shape leads to hysteresis. This simple molecular model is able to predict the change in the interface geometry without invoking the Kelvin equation or the macroscopic concept of surface tension.   **© 1998 Academic Press**

Key Words: adsorption equilibria; lattice theory; hysteresis; porous materials.

INTRODUCTION

Adsorption on porous solids is an important phenomenon for many practical applications, including purification of gases (1) and liquids (2), decolorizing sugar (3), chromatography (4), membrane technology (5), and catalysis (6). Classical models for adsorption of single-component gas (7–9) consider monolayer behavior (in particular, the Langmuir and Frumkin models (10, 11)) or a semi-infinite adsorbate at a flat boundary (for example, the BET (12) and Frenkel–Halsey–Hill models (13–15)). The pore structures of adsorbent materials have been taken into account by empirical approaches such as Polanyi theory (16), its various modifications (17), and by fractal analysis (18). However, these empirical theories do not describe hysteresis due to differences between the adsorption and desorption branches of the isotherms (7, 8). To describe hysteresis, these empirical models need an additional equation (such as the Kelvin equation) which does not come from the adsorption model. This additional equation contains additional parameters (such as surface tension and contact angle).

The classical model of adsorption hysteresis (7) is based on considering a pore of some shape (say, cylindrical of radius r).

In the adsorption branch of the isotherm, there is monolayer adsorption on the wall of the pore for small pressures. Increasing pressure causes multilayer adsorption and eventually condensation of the adsorbate. During desorption, the geometry of the interface is assumed to be different, as illustrated in Fig. 1. In this case, the desorption branch is different because the pressure during evaporation from the meniscus, p, given by the Kelvin equation (7),

$$\ln \frac{p}{p_s} = -\frac{2\gamma V}{rRT} \cos \phi, \qquad [1]$$

is different from the saturation vapor pressure, p_s. In this equation γ is the surface tension and V is the molar volume of the liquid adsorbate; ϕ is the contact angle between the liquid and the wall of the pore; R is the universal gas constant, and T is the absolute temperature. In other words, adsorption occurs at $p = p_s$ and $r = \infty$, but desorption occurs for a small r and at $p < p_s$ given by Eq. [1]. Though the statistical mechanical foundations of the Kelvin equation have been analyzed in detail (9), its application to the qualitative interpretation of adsorption hysteresis has been empirical (7, 8).

The current IUPAC classification of adsorption isotherms (19) gives four types of hysteresis loops designated as H1, H2, H3, and H4. These types are illustrated in Fig. 2. Types H1 and H4 are characterized as the "extreme types" where branches are "almost vertical (H1) and nearly parallel (H4) over an appreciable range of gas uptake" (19). Types H2 and H3 are "intermediate between these two extremes." However, this characterization does not relate the shape of hysteresis loops to the fundamental parameters of adsorption (such as pore size and molecule–molecule and molecule–surface interactions) because "the effect of various factors on adsorption hysteresis is not fully understood" (19, p. 613).

Modern methods (simulations (20), density functional theory (21–23), self-consistent field theory (24)), are able, in principle, to predict adsorption hysteresis without invoking the Kelvin equation. However, these methods do not give analytical solutions and they require tedious numerical calculations. Consequently, there never has been a rigorous, systematic analysis of hysteresis behavior.

Here we present an analysis of adsorption hysteresis using lattice theory concepts based on ideas of Ono and Kondo (25).

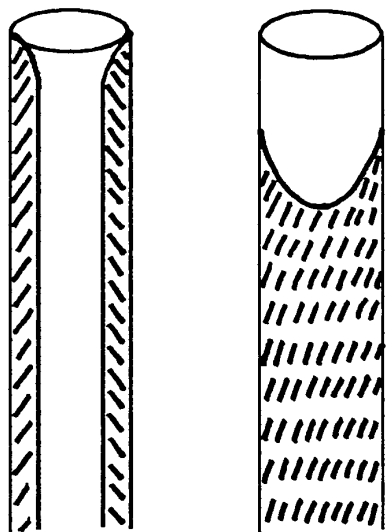
[1] To whom correspondence should be addressed.

FIG. 1. Classical model of adsorption and desorption in pores.

The Ono–Kondo approach originally was derived as a one-dimensional theory for a semi-infinite fluid with a flat boundary to describe density gradients at vapor–liquid (26) and liquid–solid (27) interfaces. Recently, this approach has been generalized to three dimensions (28). This generalization allows one to describe adsorption equilibria for arbitrary boundary condi-
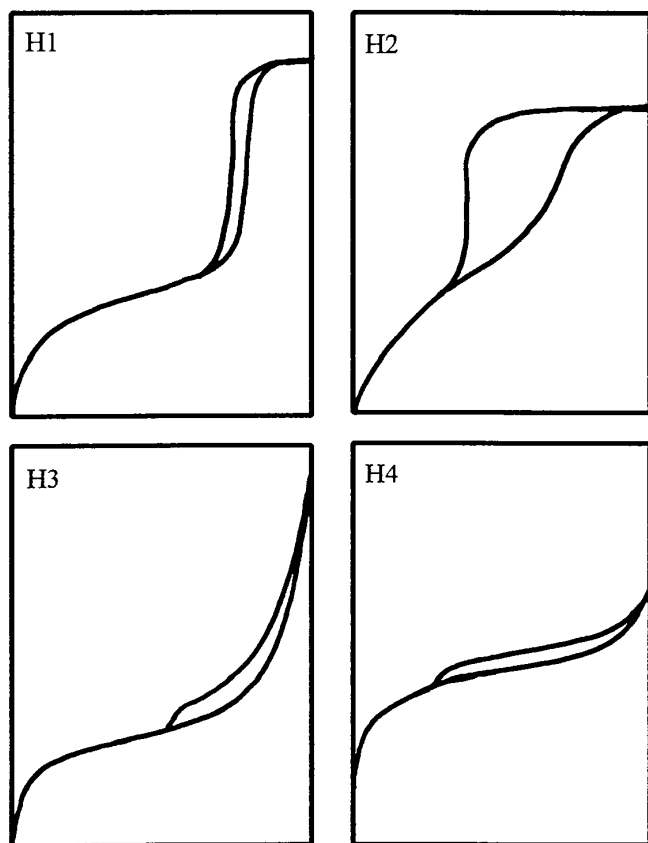

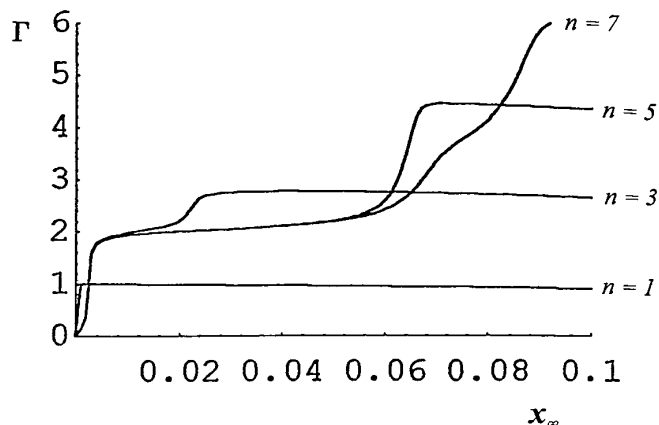**FIG. 2.** The current IUPAC classification of hysteresis loops.

FIG. 3. The Gibbs adsorption isotherms in infinite-size slit-like pores for $\epsilon/k_BT = 1.0$, $\epsilon_s/k_BT = 4.0$, and different pore widths, n.

tions. In this paper, this new approach is used to analyze adsorption hysteresis in slit-like pores.

LATTICE MODEL

Here we consider lattice theory for a one-component fluid where i, j, and k are the three dimensions of the lattice coordinates. We assume that the lattice fluid is in contact with the walls of a porous adsorbent. There are interactions between nearest neighbors with ϵ being the energy of adsorbate–adsor-
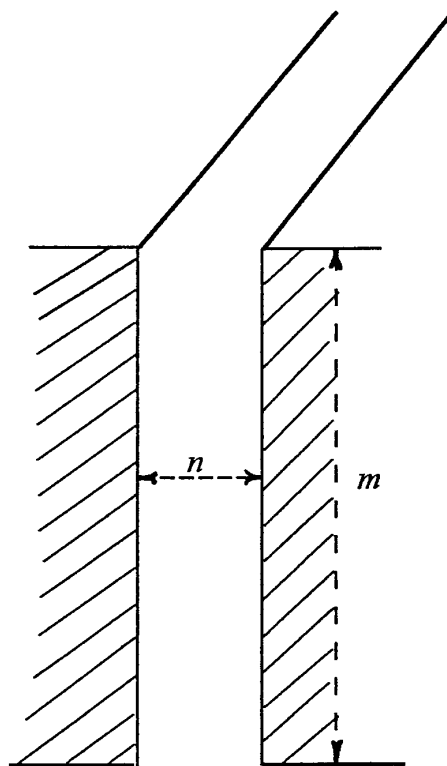

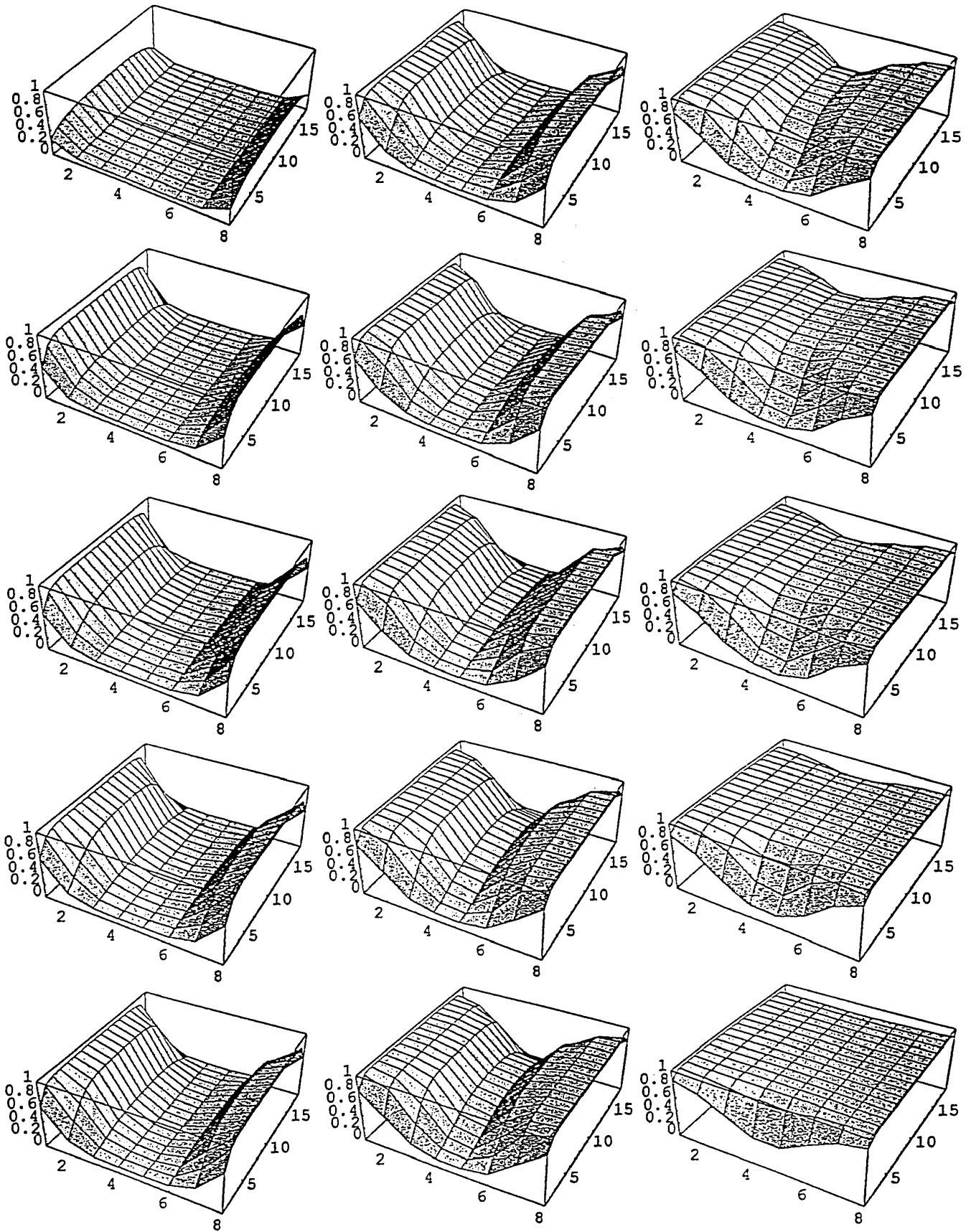**FIG. 4.** Finite-width, finite-length slit-like pore.

FIG. 5. Adsorption in finite-size, slit-like pore for $\epsilon/k_B T = \epsilon_s/k_B T = 1.0$.
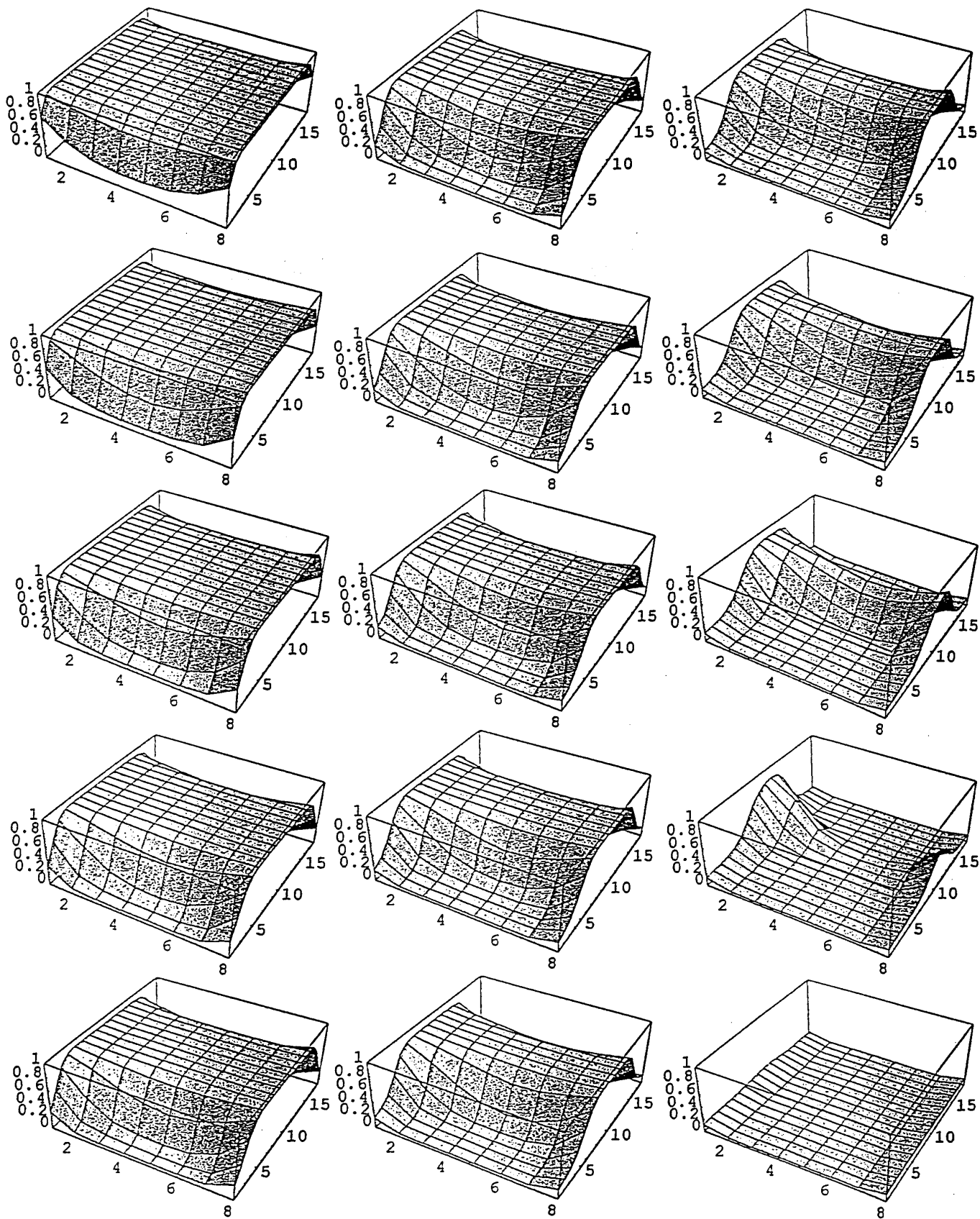
FIG. 6. Desorption in finite-size, slit-like pore for $\epsilon/k_B T = \epsilon_s/k_B T = 1.0$.
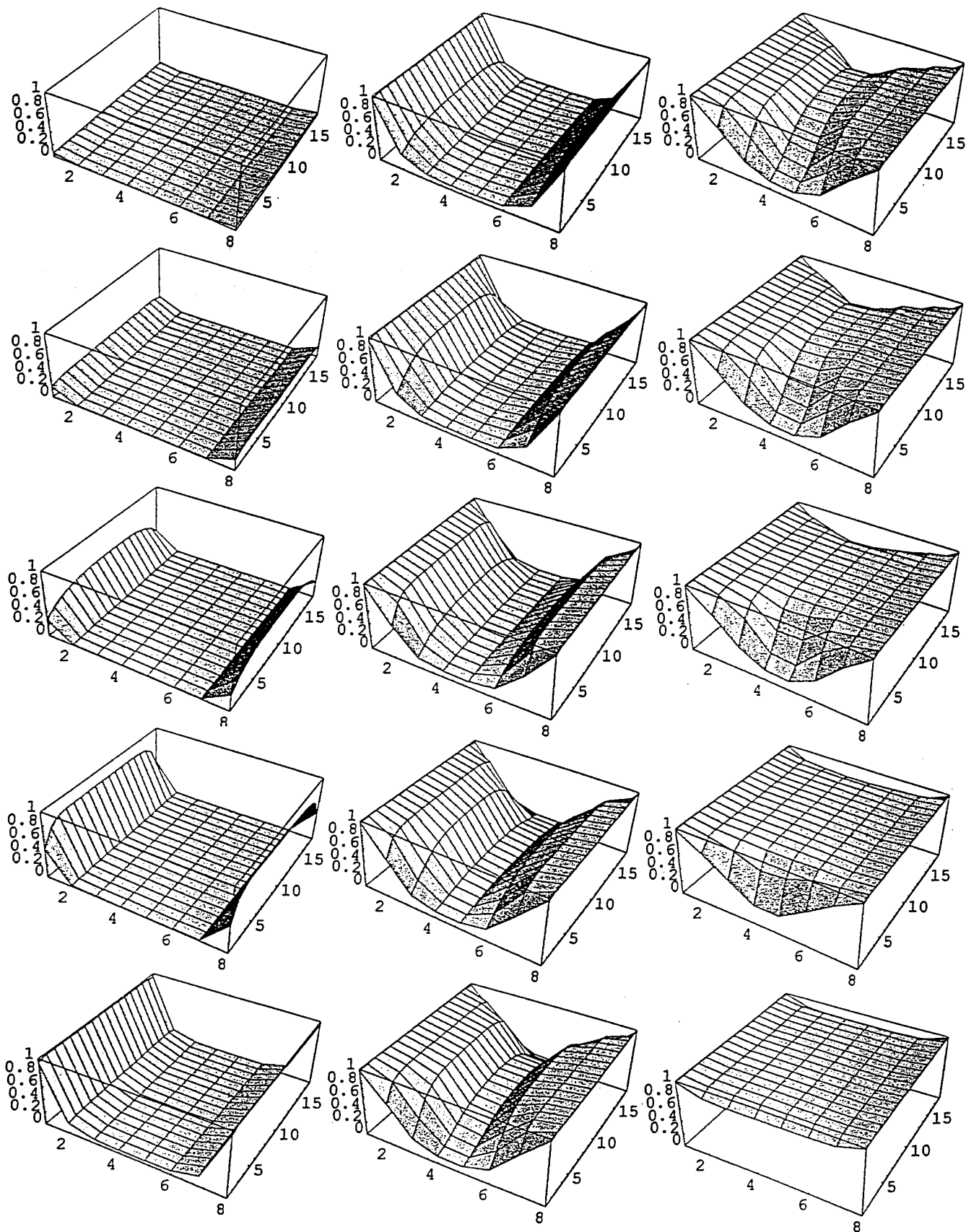
FIG. 7. Adsorption in finite-size, slit-like pore for $\epsilon/k_BT = 1.0$ and $\epsilon_s/k_BT = 3.0$.
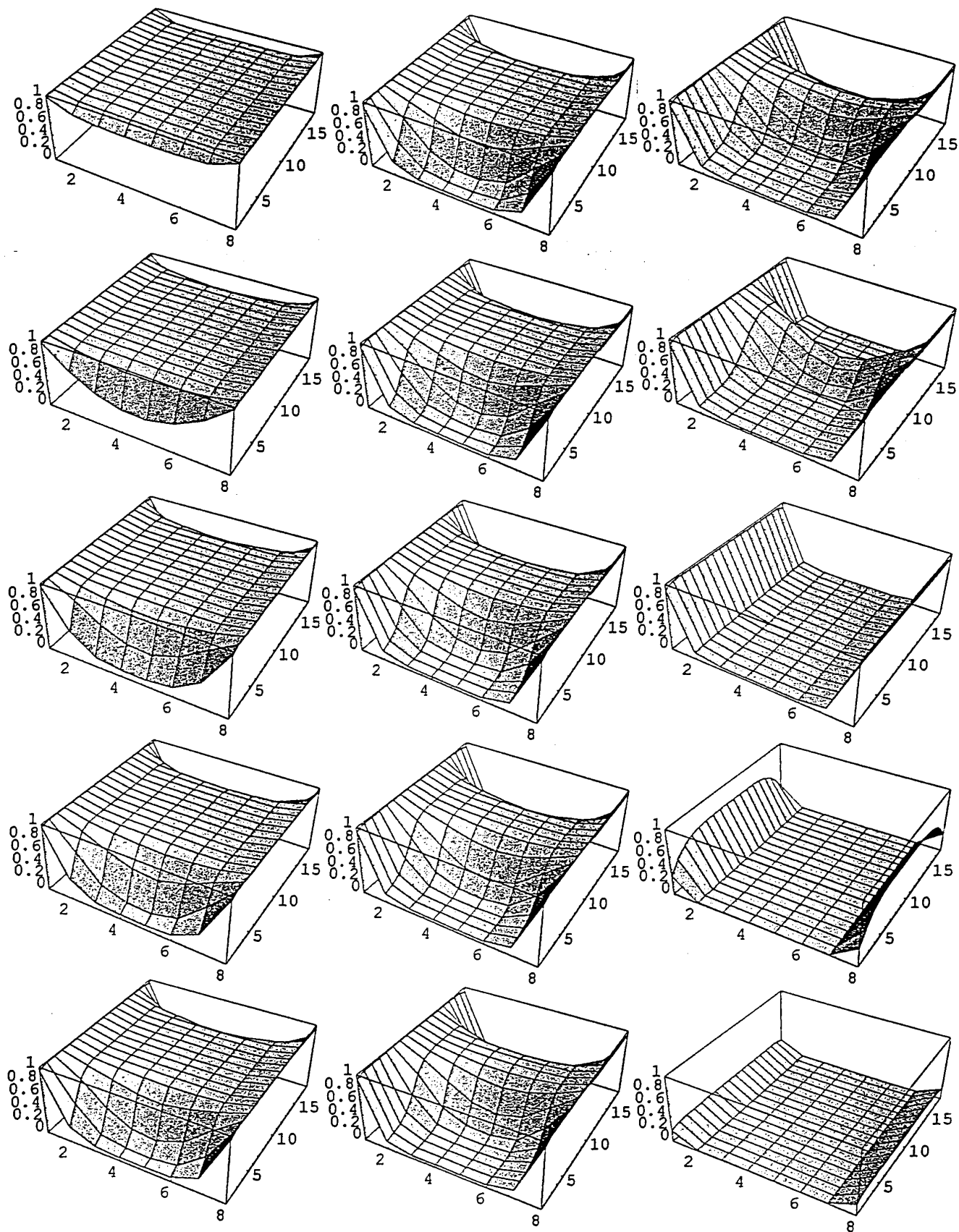
FIG. 8. Desorption in finite-size, slit-like pore for $\epsilon/k_B T = 1.0$ and $\epsilon_s/k_B T = 3.0$.
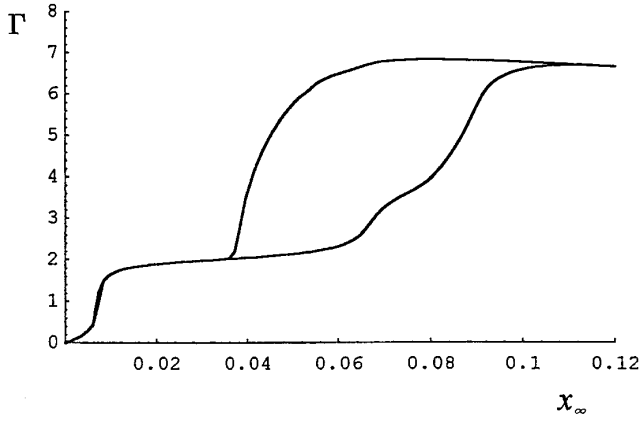
FIG. 9. Isotherm of the Gibbs adsorption for $\epsilon/k_B T = 1.0$ and $\epsilon_s/k_B T = 3.0$.

bate interactions, and ϵ_S being the energy for adsorbate–surface interactions.

The classical Ono–Kondo theory of thermodynamic equilibrium for a semi-infinite adsorbate at a flat boundary gives a one-dimensional density distribution near the surface. For a porous adsorbent, it is necessary to consider the Ono–Kondo equations in three dimensions and to couple them to boundary conditions that describe the surface (energy) topology.

Consider taking an adsorbate molecule at a site with coordinates i, j, k and moving it to an empty site in the bulk (outside the pore). This is equivalent to the exchange of a molecule with a vacancy,

$$A_{i,j,k} + V_\infty \rightarrow V_{i,j,k} + A_\infty, \qquad [2]$$
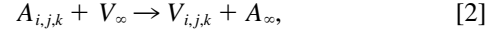
where A is the adsorbate molecule and V is the vacancy (empty site) that it fills (and vice versa). If this exchange occurs at equilibrium, then

$$\Delta H - T\Delta S = 0, \qquad [3]$$

where ΔH and ΔS are the enthalpy and entropy changes, and T is the absolute temperature.

Value of ΔS can be represented in the form

$$\Delta S = k_B \ln W_1 - k_B \ln W_2, \qquad [4]$$

where W_1 is the number of configurations where the site with coordinates i, j, k is occupied by an adsorbate molecule and the infinitely distant site is empty, and W_2 is the number of configurations where the infinitely distant site is occupied by an adsorbate molecule and the site with coordinates i, j, k is empty. Here k_B is Boltzmann's constant.
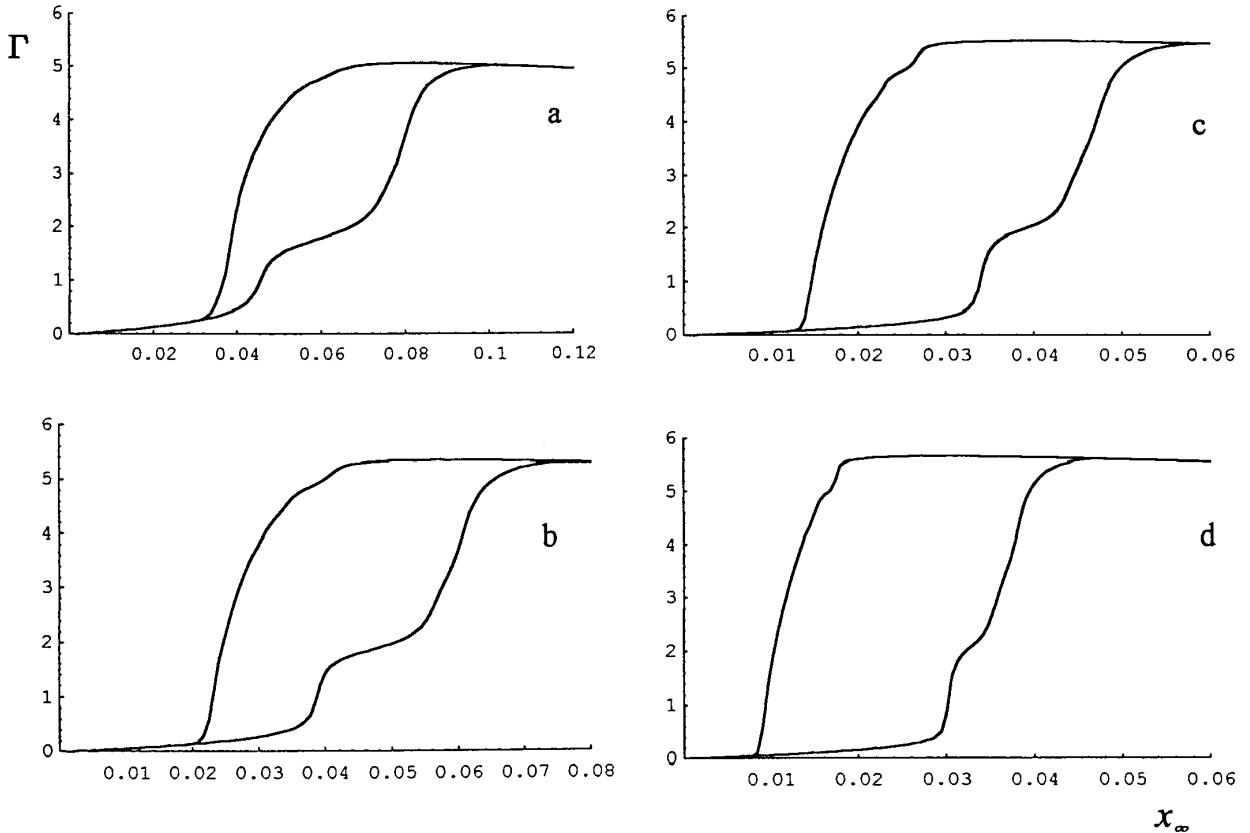

FIG. 10. The Gibbs adsorption isotherms for $m = 18$, $n = 8$, $\epsilon_s/k_B T = 1.3$, and different $\epsilon/k_B T$: 1.0 (a), 1.1 (b), 1.2 (c), and 1.3 (d).
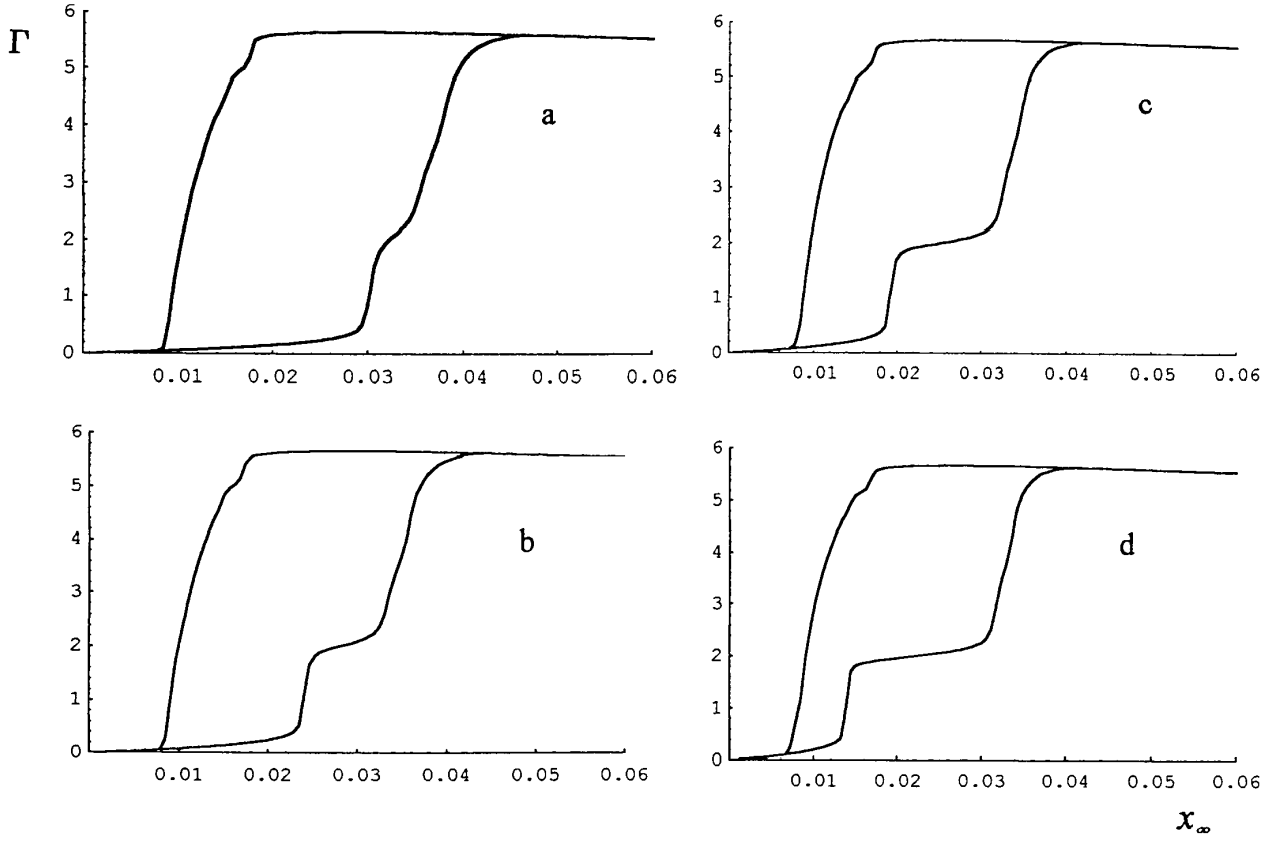
FIG. 11. The Gibbs adsorption isotherms for $m = 18$, $n = 8$, $\epsilon/k_B T = 1.3$, and different $\epsilon_s/k_B T$: 1.3 (a), 1.5 (b), 1.7 (c), and 2.0 (d).

If the overall number of configurations for the system is W_0, then in mean-field lattice approximation

$$W_1/W_0 = x_{i,j,k}(1 - x_\infty) \qquad [5]$$

and

$$W_2/W_0 = (1 - x_{i,j,k})x_\infty, \qquad [6]$$

where $x_{i,j,k}$ is the probability that the site with coordinates i, j, k is occupied by an adsorbate molecule, and x_∞ is the bulk mole fraction of adsorbate.

Substituting Eqs. [5] and [6] into Eq. [4] we have

$$\Delta S = k_B \ln\{[x_{i,j,k}(1 - x_\infty)]/[(1 - x_{i,j,k})x_\infty]\}. \qquad [7]$$

The change in enthalpy can be calculated in the mean-field approximation for a simple cubic lattice by considering the number of neighboring sites that are occupied near the surface compared to the bulk. Then,

$$\Delta H = -(x_{i+1,j,k} + x_{i-1,j,k} + x_{i,j+1,k} + x_{i,j-1,k}$$
$$+ x_{i,j,k+1} + x_{i,j,k-1} - 6x_\infty)\epsilon. \qquad [8]$$

From Eq. [3] and Eqs. [7] and [8] it follows that

$$\ln\{[x_{i,j,k}(1 - x_\infty)]/[(1 - x_{i,j,k})x_\infty]\}$$
$$+ (x_{i+1,j,k} + x_{i-1,j,k} + x_{i,j+1,k} + x_{i,j-1,k}$$
$$+ x_{i,j,k+1} + x_{i,j,k-1} - 6x_\infty)\epsilon/k_B T = 0. \qquad [9]$$

Equation [9] is the Ono–Kondo equation for three dimensions. It relates the local density in each site (i, j, k) to the density in the bulk.

NUMERICAL CALCULATIONS

Boundary Conditions

Obtaining the density distribution from Eq. [9] requires appropriate boundary conditions. Consider the exchange given in Eq. [2] for a molecule at the surface. Then, instead of Eq. [9], we get

$$\ln\{[x_s(1 - x_\infty)]/[(1 - x_s)x_\infty]\}$$
$$+ (\sum_{q=1}^{N} x_{sq} - 6x_\infty)\epsilon/k_B T + M\epsilon_s/k_B T = 0, \qquad [10]$$

where x_s is the probability that the site on the surface is occupied by an adsorbate molecule ($s = \{i, j, k\}$ for sites on the surface), x_{sq} is the probability that the qth neighboring site is occupied by an adsorbate molecule ($sq = \{i \pm 1, j \pm 1, k \pm 1\}$ for possible neighbors of the s site), M is the number of bonds between a molecule and surface, and N is the coordination number for molecules on the surface.

The boundary condition given in Eq. [10] was to calculate density distributions in slit-like pores. This density distribution leads to the Gibbs adsorption, Γ,

$$\Gamma = \sum_{\Omega} (x_{i,j,k} - x_\infty), \qquad [11]$$

where summation is done over the entire volume of the pore(s), Ω.

Equation [11] is the adsorption isotherm representing the Gibbs adsorption versus the reduced density, x_∞. For one-component gas, the density is a function of pressure and temperature,

$$x_\infty = f(p, T), \qquad [12]$$

where f is the equation of state for the one-component gas. For an ideal gas, $x_\infty = p/RT$.

Infinite Slit-Like Pores

Consider a finite-width, slit-like pore with infinite walls. The width of the pore can be characterized by the number of layers, n, between walls. Because of symmetry, Eqs. [9] and [10] give only one equation for $n = 1$ and $n = 2$. For a one-layer pore this equation can be written as

$$\ln\{[x_1(1 - x_\infty)]/[(1 - x_1)x_\infty]\}$$
$$+ (4x_1 - 6x_\infty)\epsilon/k_BT + 2\epsilon_s/k_BT = 0, \quad [13]$$

where x_1 is the probability that a site in the pore is occupied by an adsorbate molecule. For a two-layer pore, this equation has the following form:

$$\ln\{[x_1(1 - x_\infty)]/[(1 - x_1)x_\infty]\}$$
$$+ (5x_1 - 6x_\infty)\epsilon/k_BT + \epsilon_s/k_BT = 0. \quad [14]$$

For $n = 3$, Eqs. [9] and [10] yield the set of equations

$$\ln\{[x_1(1 - x_\infty)]/[(1 - x_1)x_\infty]\}$$
$$+ (x_2 + 4x_1 - 6x_\infty)\epsilon/k_BT + \epsilon_s/k_BT = 0 \quad [15]$$

$$\ln\{[x_2(1 - x_\infty)]/[(1 - x_2)x_\infty]\}$$
$$+ (2x_1 + 4x_2 - 6x_\infty)\epsilon/k_BT = 0, \quad [16]$$

where x_2 characterizes the composition in the second (central) layer.

In general, for arbitrary value of n, we have Eq. [15] as a boundary condition and the coupled equations

$$\ln\{[x_i(1 - x_\infty)]/[(1 - x_i)x_\infty]\}$$
$$+ (x_{i-1} + 4x_i + x_{i+1} - 6x_\infty)\epsilon/k_BT = 0, \quad [17]$$

where $2 \leq i \leq n - 1$. In addition, we have the condition of symmetry

$$x_i = x_{n-i+1}. \qquad [18]$$

Figure 3 illustrates the Gibbs adsorption isotherms calculated from Eqs. [11], [14], and [17] for different pore widths, n. As illustrated in Fig. 3, the isotherms can have steps resulting from two-dimensional phase transitions in layers. These phase transitions could exhibit hysteresis in kinetically controlled experiments. However, there is no hysteresis in the equilibrium behavior for infinite pores.

Finite-Length, Slit Pores

There are a wide variety of different boundary conditions that can be applied to Eq. [9]. These conditions can take into account surface heterogeneity (as in Ref. (28)), or they can reflect the three-dimensional geometry of the pore structure. Here we consider the simplest example of a finite pore. Consider a pore with n being the width (in the units of numbers of layers) in the i direction and m being the length of pore walls in the j direction. The pore is infinite in the k direction as illustrated in Fig. 4. This geometry implies that there is an energy of molecule–surface interaction, ϵ_s, at the sites where $0 < j < m + 1$. Also we assume $x_{i,0,k} = x_{i,m+1,k} = x_\infty$ for any i and k. Numerical solutions of Eq. [9] with these conditions were found by the method of successive substitutions (29, Section 20.2.2).

Figures 5 and 6 demonstrate different behavior for adsorption and desorption at $\epsilon/k_BT = \epsilon_s/k_BT = 1.0$ for a pore 8 molecular diameters wide and 18 molecular diameters long. Though the results shown in Figs. 5 and 6 are calculated with the same set of coupled equations, the adsorption and desorption behaviors differ because of the different initial conditions. For adsorption, the calculations start from zero density and the adsorption is calculated as the density increases. This leads to growth in a layer-by-layer fashion on the walls. For desorption, the calculations start with the pore filled by the adsorption process and desorption occurs as the external pressure or density is decreased. During desorption, the evaporation also occurs in a layer-by-layer fashion, but from the ends of the pore inward.

Figures 7 and 8 show adsorption and desorption at $\epsilon/k_BT = 1.0$, and $\epsilon_s/k_BT = 3.0$. Here the molecule–surface interactions are much stronger than in Figs. 5 and 6. During adsorption,

layers grow on walls, eventually filling the pore volume (Fig. 7). During desorption, evaporation of molecules occurs from the free surfaces, and only near the end of the desorption process are there layers on the walls (Fig. 8). Figure 9 illustrates the Gibbs adsorption isotherm for the processes shown in Figs. 7 and 8. As seen from Fig. 9, there is a hysteresis loop indicating different behavior during adsorption and desorption.

Figure 10 shows the Gibbs adsorption isotherms for $m = 18$, $n = 8$, $\epsilon_s/k_BT = 1.3$, and different ϵ/k_BT: 1.0 (a), 1.1 (b), 1.2 (c), and 1.3 (d). As seen from Fig. 10, the edges of the hysteresis loop become steeper as ϵ/k_BT goes up. Figure 11 illustrates the Gibbs adsorption isotherms for $m = 18$, $n = 8$, $\epsilon/k_BT = 1.3$, and different ϵ_s/k_BT: 1.3 (a), 1.5 (b), 1.7 (c), and 2.0 (d). As seen from Fig. 11, the shape of the adsorption branch changes dramatically from relatively smooth monotonic behavior (at $\epsilon_s/k_BT = 1.3$) to stepped behavior (at $\epsilon_s/k_BT = 2.0$).

CONCLUSION

The Ono–Kondo lattice theory with appropriate boundary conditions is able to predict adsorption hysteresis for fluid in semi-finite, slit-like pores. It is shown that there can be phase transitions in the adsorbed phase which lead to hysteresis in kinetically controlled experiments. However, hysteresis in equilibrium behavior is exhibited only in pores of finite length. For finite-length pores, the interface geometry is predicted to be different during the processes of adsorption and desorption, and this difference in interface shape leads to hysteresis.

This simple molecular model is able to predict the change in the interface geometry without invoking the Kelvin equation or the macroscopic concept of surface tension.

ACKNOWLEDGMENTS

REFERENCES

1. Keller, G. E., *Chem. Eng. Prog.* **11,** 56 (1995).
2. Deng, X., Yue, Y., and Gao, Z., *J. Colloid Interface Sci.* **192,** 475 (1997); Samuel, D. F., and Osman, M. A., "Adsorption Processes for Water Treatment." Butterworth, Stoneham, MA, 1987.
3. Robens, E., *in* "Studies in Surface Science and Catalysis," (J. Rouquerol, F. Rodríguez–Reinoso, K.S.W. Sing and K. K. Unger, Eds.), p. 109. Elsevier Science, Amsterdam, New York, 1994.
4. Helfferich, F. G., *J. Chromatogr. A* **768,** 169 (1997).
5. Munoz-Aguardo, M.-J., and Gregorkiewitz, M., *J. Colloid Interface Sci.* **185,** 459 (1997); Uemiya, S., Kajiwara, M., and Kojima, T., *AIChE J.* **43,** 2715 (1997).
6. Mehandjiev, D., Bekyarova, and Khristova, M., *J. Colloid Interface Sci.* **192,** 440 (1997).
7. Gregg, S. J., and Sing, K. S. W., "Adsorption, Surface Area and Porosity." Academic Press, London, 1982.
8. Jaycock, M. J., and Parfitt, G. D., "Chemistry of Interfaces." Wiley, New York, 1981; Adamson, A. W., "Physical Chemistry of Surfaces." Wiley, New York, 1976.
9. Rowlinson, J. S., and Widom, B., "Molecular Theory of Capillarity." Clarendon, Oxford, 1982.
10. Langmuir, I., *J. Am. Chem. Soc.* **39,** 1848 (1917).
11. Frumkin, A., *Z. Phys. Chem. (Leipzig)* **116,** 466 (1925).
12. Brunauer, S., Emmett, P. H., and Teller, E., *J. Am. Chem. Soc.* **60,** 309 (1938).
13. Frenkel, Y. I., "Kinetic Theory of Liquids." Clarendon, Oxford, 1946.
14. Halsey, G. D., *J. Chem. Phys.* **16,** 931 (1948).
15. Hill, T. L., *Adv. Catal.* **4,** 211 (1952); Hill, T. L., *J. Am. Chem. Soc.* **72,** 5347 (1950).
16. Polanyi, M., *Verh. Deutsche Phys. Ges.* **Bd. 16,** S.1012 (1914); *Trans. Faraday Soc.* **28,** 316 (1932).
17. Stoeckli, H. F., Huguenin, D., and Laederach, A., *Carbon* **32,** 1359 (1994); Sundaram, N., *Langmuir* **11,** 3223 (1995).
18. Sermob, P. A., Wang, Y., and Vong, M. S. W., *J. Colloid Interface Sci.* **168,** 327 (1994).
19. IUPAC Commission on Colloid and Surface Chemistry Including Catalysis, *Pure Appl. Chem.* **57,** 603 (1985). ["Reporting Physisorption Data for Gas/Solid Systems with Special Reference to the Determination of Surface Area and Porosity"]
20. Bojan, M. J., Vernov, A. V., and Steele, W. A., *Langmuir* **8,** 901 (1992); Razmus, D. M., and Hall, C. K., *AIChE J.* **37,** 769 (1991).
21. Lastoskie, C., Gubbins, K. E., and Quirke, N., *J. Phys. Chem.* **97,** 4786 (1993).
22. Olivier, J. P., *J. Porous Mater.* **2,** 9 (1995).
23. Ravikovitch, P. I., Domhnaill, S. C. O., Neimark, A. V., Schuth, F., and Unger, K. K., *Langmuir* **11,** 4765 (1995).
24. Schlangen, L. J. M., and Koopal, L. K., *Langmuir* **12,** 1863 (1996).
25. Ono, S., and Kondo, S., *in* "Encyclopedia of Physics" (S. Flügge, Ed.), Vol. 10, p. 134. Springer-Verlag, Berlin/Gottingen/Heidelberg, 1960.
26. Rowlinson, J. S., and Widom, B., "Molecular Theory of Capillarity." Clarendon, Oxford, 1982; Lane, J. E., and Johnson, C. H. J., *Aust. J. Chem.* **20,** 611 (1967).
27. Lane, J. E., *Aust. J. Chem.* **21,** 827 (1968); Altenberger, A. R., and Stecki, J., *Chem. Phys. Letters* **5,** 29 (1970).
28. Aranovich, G. L., and Donohue, M. D., *J. Chem. Phys.* **104**(10), 3851 (1996).
29. Korn, G. A., and Korn, T. M., "Mathematical Handbook for Scientists and Engineers.'' McGraw–Hill, New York, 1961.